7th Asian International Seminar on Atomic and Molecular Physics IOP Publishing
Journal of Physics: Conference Series **80** (2007) 012002 doi:10.1088/1742-6596/80/1/012002

Core-excitation effects on atomic transitions

T. N. Chang[1,2] and Yuxiang Luo[1]

[1] Department of Physics and Astronomy, University of Southern California, Los Angeles, CA 90089-0484, U.S.A.

[2] National Center for Theoretical Sciences, Hsinchu, Taiwan, 30039, ROC

Email: tnchang@usc.edu

Abstract. By including explicitly the electronic configurations with three simultaneously excited electronic orbitals, we have successfully extended the BSCI (B-spline based configuration interaction) method to estimate directly the effects of inner shell core-excitation to atomic transitions. In particular, we are able to carry out detailed *ab initio* investigation on the core polarization effects without the need of employing parameterized model potential. We present in this paper quantitatively the change in atomic transition rate due to the core excitations for four-electron systems, especially for transitions involving doubly excited states and transitions with small oscillator strengths. Our numerical results using length and velocity gauge typically agree to better than 1% .

PACS code: 32.70.Cs; 32.70.Fw; 31.15.Ar; 31.25.Jf

1. Introduction

For atomic systems with two or more actively interacting electrons and also for transitions involving doubly excited bound states or excited states with higher effective principal quantum number, a detailed high precision theoretical characterization of atomic transitions, both in terms of the oscillator strength and the excitation energy determined by the energy difference between the initial and final states of the transition, remains a theoretical challenge to atomic structure theory. Some of the most accurate theoretical calculations, e.g., the multiconfiguration Hartree-Fock (MCHF) method by Froese Fischer and her co-workers [1, 2], are able to estimate consistently the oscillator strengths for transitions between low lying excited atomic

states with an agreement between the length and velocity results to less than 1% or much better.

In this paper, we present an extension of the B-spline based configuration interaction (BSCI) methods [3, 4] to include explicitly the effects due to the interactions beyond those between the two strongly interacting outer electrons. With the exception of applications to two-electron systems, the previous BSCI calculations have employed the parametrized model potentials such as the ones with the expressions given by Eqs. (19) and (20) in [3] to emulate the core-excitation effects (or core polarized interactions). Unlike some of the atomic structure theories, which are carried out individually for each energy eigenstate in separate calculation, the BSCI calculation, depending upon the size of the radius R of the interacting sphere, has the advantage to evaluate in one single calculation the energy eigenvalues and oscillator strengths for a large number of excited states as long as their electronic orbits are confined in the sphere. In spite of the success of the BSCI approach to understand both qualitatively and quantitatively the atomic transitions, including the photoionization to the continuum dominated by the doubly excited autoionization resonances, there are a number of basic difficulties that one needs to address. One of the key questions is if the use of model potentials can adequately account for the core-excitation effect. Since the use of model potentials unavoidably leads to difference between the length and velocity results even when the basis functions are extended to exhaust all possible configurations (including those from the continuum) corresponding to the excitations of two interacting electrons (see, e.g., [5]), can one estimate the uncertainty due to such approximation? The second key question is the use of large basis functions in the BSCI calculation, i.e., what would be the computational requirement if one goes beyond the basis functions which limit to those with only two electrons simultaneously in the excited orbitals?

To effectively deal with those difficulties, we first extend in this work the BSCI method to study in details the core-excitation effects with one of the inner shell electrons occupying an excited orbit, together with the two strongly interacting outer electrons. The calculations are carried out without the use of model potentials such as the ones that simulate the long-range core polarizations. Theoretical considerations aside, the extension of BSCI method to include explicitly the core-excitation effects requires substantially more computational effort than other L^2 methods. The high performance parallel computing environment available in recent years has opened up the door for such a theoretical approach to estimate quantitatively the atomic transition data with high precision.

2. Key theoretical features

The Hamiltonian matrix in the present extended BSCI calculation is generated

using basis functions that represent electronic configurations corresponding to two and three electrons in the excited orbitals. Specifically, in the application to the four-electron systems presented in this paper, we include two types of electronic configurations, i.e., a) $((1s^2)^1S\ (nln'l')^{SL})^{SL}$ and b) $([(1snl)^{S_{12}L_{12}}][(n_1l_1n_2l_2)^{S_{34}L_{34}}])^{SL}$. By including the $l = 0, 1$, and 2 orbitals in the type b) configurations, we are able to take into account explicitly the core-excitation (or, core polarization) effects represented by the excitation of one of the inner $1s$ electrons into all the s, p, and d excited orbitals. Our BSCI calculation, using the quasi-complete set of one-electron basis set expanded with B-splnes, includes both negative energy (bound) orbitals and the positive energy (continuum) orbitals. In addition to the configurations representing two equivalent electrons nl^2, which we include in all BSCI calculation, we have also focused our investigation on the effect to atomic transitions due to the contribution from three equivalent electrons, i.e., a type c) configuration $(1s(np^3)^{S'L'})^{SL}$. By including explicitly the types b) and c) configurations in our calculation to account for the core excitation, the BSCI calculation no longer requires the parameterized model potentials such as the ones represented by Eqs. (19) and (20) in [3]. Detailed expressions for the Hamiltonian matrix elements between all three types of configurations a), b) and c) are given elsewhere [6].

The computational effort required in the present work is substantial. In a typical L^2 calculation (e.g., MCHF calculation), the pseudostates with variational parameters to represent orbitals for each angular momentum are relatively small, e.g., often less than ten. For configurations with three electrons in the excited orbitals, the total number of basis functions are generally smaller than 1000 for each combination of three corresponding one-electron orbital angular momenta. As a result, such calculation can be carried out easily with a Hamiltonian matrix of a size less than a few thousands. In an extended BSCI calculation, instead, the size of each quasi-complete set of one-electron orbitals are typically of the order of 30 or more. As a result, with the product of three actively interacting electrons and with various combinations of three one-electron orbital angular momenta, the size of the Hamiltonian matrix may exceed 2×10^5 by 2×10^5 in a typical calculation.

In addition, the use of atomic orbitals in BSCI calculation leads to a Hamiltonian matrix that is non-sparse. Since most of the existing matrix diagonalization codes for large matrix essentially work only for the sparse matrix, we rely on the two-step diagonalization procedure outlined in [3] for the BSCI calculation. As high as 200 GB of total memory could be required for the Hamiltonian matrix when it is stored distributively in parallel computing system for the two-step diagonalization procedure. Our codes are designed to calculate the energy eigenvalue and its corresponding eigenvector for each energy eigenstate individually. The resulting eigenvectors typically have an orthogonality of 10^{-7} or better in spite of their large size. The ability to perform effectively the large-scale numerical calculation also opens up the possibility to

study systematically the improvement of the agreement between length and velocity results for the oscillator strengths as we include additional interactions in the BSCI calculations.

By systematically adding more core-excitation effects into the theoretical calculation, we are in a position to examine the qualitative argument that the transition rate (e.g., the oscillator strength) could be more readily estimated from the dipole length approximation since the radial dipole matrix relies less on the quality of the orbital functions at small r region where electron correlation dominates. In other words, we want to address the question that to what extent one needs to take into account in great details the strong short range electronic correlation in length calculation since the estimated transition rate from the length results may already be fairly reliable in the absence of more elaborate calculations. To support such a qualitative argument, it is essential to demonstrate that the calculated oscillator strength with velocity gauge indeed converges to the length result when the multielectron interactions responsible for the short range correlation (e.g., the core-excitation effect) are explicitly included in the detailed theoretical calculations.

It is also necessary to pay additional care when estimating the oscillator strengths for atomic systems alone the isoelectronic sequence due to the "plunging" of the doubly excited bound states into the series of singly excited bound states as the effective nuclear charge Z increases [7]. The strong mixing due to the close proximity of the doubly and singly excited bound states often affects substantially the oscillator strengths, which may lead to strong variation for a specific transition along the isoelectronic sequence as a function of Z and also for a series of transitions along the singly excited bound series as the effective principal quantum number increases. The usual small oscillator strengths for transition from singly excited to doubly excited bound states involving simultaneous change of two electronic orbitals may also be enhanced.

Figure 1 illustrates the plunging of the doubly excited $2pnd\ ^3F$ and $2png\ ^3F$ states into the singly excited $2s\nu f\ ^3F$ series for the Be isoelectronic sequence. The doubly excited $2p3d\ ^3F$ state first appears between the $2s4f\ ^3F$ and $2s5f\ ^3F$ states in C_{III} (Z=6). The combined effect of the doubly excited $2pnd\ ^3F$ series to the singly excited $2s\nu f\ ^3F$ series is clearly shown from the shifts of the energy eigenvalues of the $2s\nu f\ ^3F$ series of B_{II} (Z=5) for states with $\nu \geq 6$. The crossing of the $2p3d\ ^3F$ state from the higher energy side to the lower energy side of the $2s4f\ ^3F$ state from C_{III} to N_{IV} also affects strongly the energy eigenvalues of the $2s4f\ ^3F$ state. Figure 2 shows the plunging of the doubly excited $2pnp\ ^1D$ and $2pnf\ ^1D$ series into the singly excited $2s\nu d\ ^1D$ series. Similar to the ^3F energy spectra shown in Fig. 1, the quantum defects of the low lying singly excited states no longer vary along the isoelectronic sequence as Z increases when the low lying doubly excited states move into their eventual proper places. As a result, qualitatively, we expect that the corresponding oscillator strengths

should also again vary smoothly as Z increases along the isoelectronic sequence.

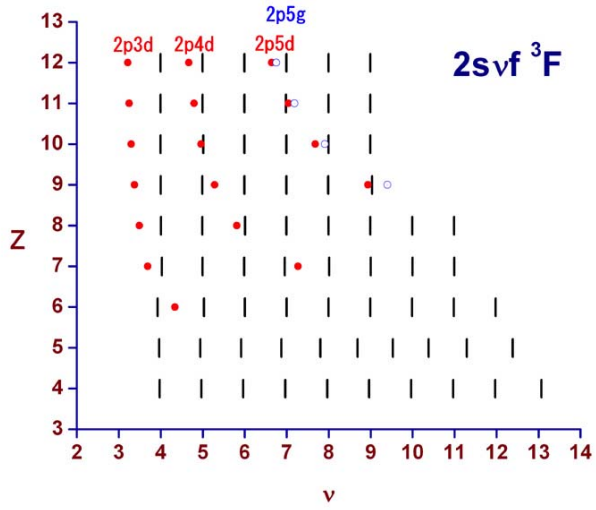

Figure 1. The calculated energy levels in terms of the principal quantum number ν against the $2s$ threshold for the singly excited $2snf\ ^3F$ states (vertical bar) and the doubly excited $2pnd\ ^3F$ (solid circle) and $2png\ ^3F$ (open circle) states for the Be isoelectronic sequence (e.g., $Z = 4$ for Be_I).

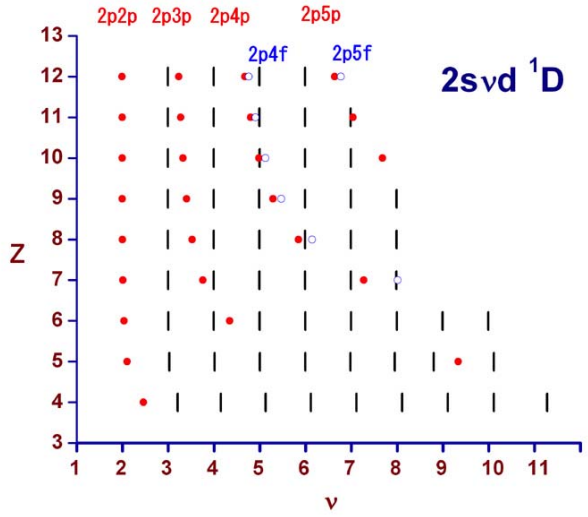

Figure 2. The calculated energy levels in terms of the principal quantum number ν for the singly excited $2snd\ ^1D$ states (vertical bar) and the doubly excited $2pnp\ ^1D$ (solid circle) and $2pnf\ ^1D$ (open circle) states for the Be isoelectronic sequence.

3. Results and discussions

The theoretical results presented in this paper are performed at three levels of approximation. We first start with the calculation (denoted as calculation A) with only the type a) configurations, i.e., the configurations represented by $((1s^2)^1S\ (nln'l')^{SL})^{SL}$,

for the Hamiltonian matrix. Since we no longer include the model potential in calculation A as we did in our previous BSCI calculation, the core-excitation effect is completely excluded in this calculation. In the second step of our calculation (denoted as calculation B), we include, in addition to type a) configurations, also the type b) configurations (i.e., the ones represented by $([(1snl)^{S_{12}L_{12}}][(n_1l_1n_2l_2)^{S_{34}L_{34}}])^{SL}$). We should note that in type b) configurations, we have also included the configurations corresponding to two equivalent electrons, i.e., the configurations represented by $((1s(nl^2)^{S_1L_1})^{S'L_1}n'l')^{SL}$. By including the type b) configurations in calculation B, we have effectively taken into account explicitly most of the core-excitation effects. The last step of our calculation includes all those in calculation B and the configurations represented by the three equivalent electrons, i.e., type c) configurations $(1s(np^3)^{S'L'})^{SL}$. Calculation C turns out to be of critical importance to some of the transitions involving doubly excited states.

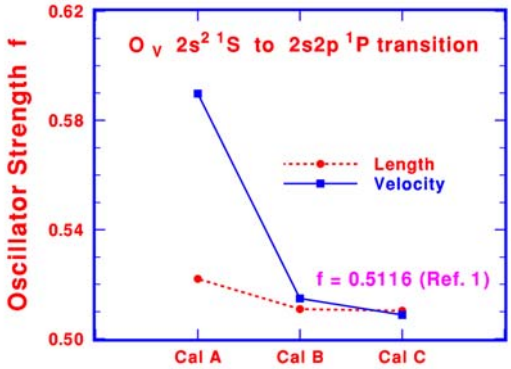

Figure 3. The changes in oscillator strengths for the $2s^2\ ^1S$ to $2s2p\ ^1P$ transitions for O_V from calculations A (in the absence of core-polarization effect) to C (with full core-excitation effect).

We start our discussion on the transition from the $2s^2\ ^1S$ ground state to the first excited $2s2p\ ^1P$ state. Figure 3 shows the calculated oscillator strengths in diploe length and velocity approximation for O_V. In the absence of the core-excitation effects, calculation A shows a more than 10% difference between the length and velocity results. With the core-excitation included in the calculation B, the agreement between length and velocity results improve to better than 1%. The effect due to the configurations corresponding to three equivalent p electrons is fairly small as shown by the calculation C. It is interesting to note that the core-excitation effects does not seem to change the length results as much as that for the velocity results. In fact, as we move along the isoelectronic sequence, our calculations have led to a similar convergence pattern as shown in Fig. 4. It appears to support the qualitative argument that the length result is not affected strongly by the short range interactions at small r region. We should point out, however, such a conclusion should not be made lightly without a more careful examination of other transitions, especially those with the initial state and the final state of the transition strongly affected by the

multielectron interactions. Our calculated results are in excellent agreement with the MCHF result by Tachiev and Froses Fischer [1].

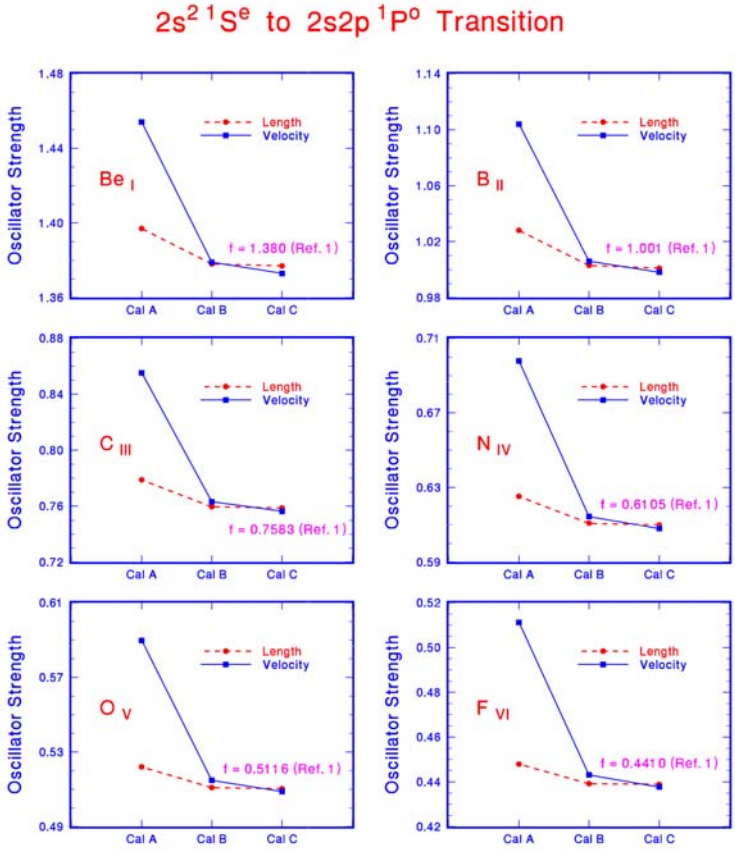

Figure 4. The convergence of the length and velocity results in oscillator strength for the $2s^2\ ^1S$ to $2s2p\ ^1P$ transitions along the Be isoelectronic sequence from calculations A (in the absence of core-polarization effect) to C (with full core-excitation effect).

The second example presented in this paper involves the transition to the first doubly excited ^1P bound state, i.e., from the $2s^2\ ^1S$ ground state to the $2p3s\ ^1P$ state. For Be_I, the $2p3s\ ^1P$ state is located above the first ionization threshold and it autoionizes into the ^1P continuum when excited. The $2p3s\ ^1P$ state plunges below the first ionization threshold in B_{II} and situates initially between the singly excited $2s5p$ and $2s6p\ ^1P$ states shown in Fig. 5. The $2p3s\ ^1P$ state plunges further along the isoelectronic sequence and eventually lies slightly above the $2s3p\ ^1P$ state as shown. Our calculation shows a strong mixing of the $2pns$ and $2snp$ configuration series for C_{III} and N_{IV} and expects an enhancement in oscillator strengths for an otherwise weak $2s^2\ ^1S \rightarrow 2p3s\ ^1P$ transition (which generally should have a relatively small transition rate due to the simultaneous change of electronic orbits of the two outer electrons). Indeed, as shown in Fig. 6, the oscillator strengths for this transition vary substantially due to the plunging of $2p3s\ ^1P$ from C_{III} to N_{IV}. The effect due to the core-excitation is illustrated in Fig. 7 for this transition in F_{VI}. The difference

between the length and velocity results is close to 20% when the core-excitation is excluded in the Calculation A. By including the core-excitation effects in Calculation B, the agreement between length and velocity results improves substantially, although it is still higher than 1%. We are able to improve the length and velocity agreement to less than 1% when the p^3 term is included in Calculation C. A clear switch over of the convergence patterns of the length and velocity results (i.e., variation from calculations A to C) from N_{IV} to O_V, is shown in Fig. 8. It reflects the completion of plunging of the $2p3s\ ^1P$ state along the isoelectronic sequence. Similar to the $2s^2\ ^1S \rightarrow 2s2p\ ^1P$ transition, the correction to the velocity results is consistently greater than that of the length results.

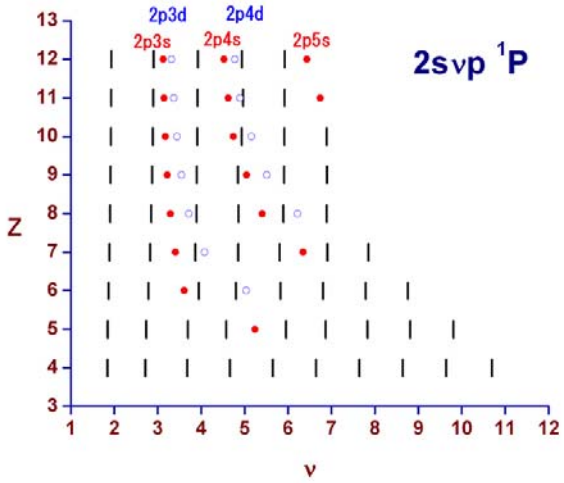

Figure 5. The calculated energy levels in terms of the principal quantum number ν for the singly excited $2snp\ ^1P$ states (vertical bar) and the doubly excited $2pns\ ^1P$ (solid circle) and $2pnd\ ^1P$ (open circle) states for the Be isoelectronic sequence.

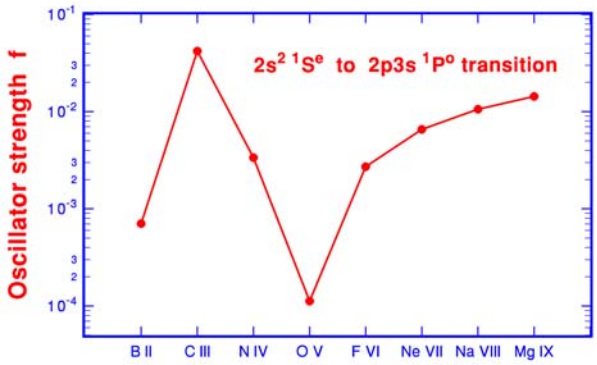

Figure 6. The variation of the oscillator strengths (from calculation C with full core-excitation effects included) for the $2s^2\ ^1S$ to $2p3s\ ^1P$ transition along the Be isoelectronic sequence. The length and velocity results are nearly identical on the log scale shown.

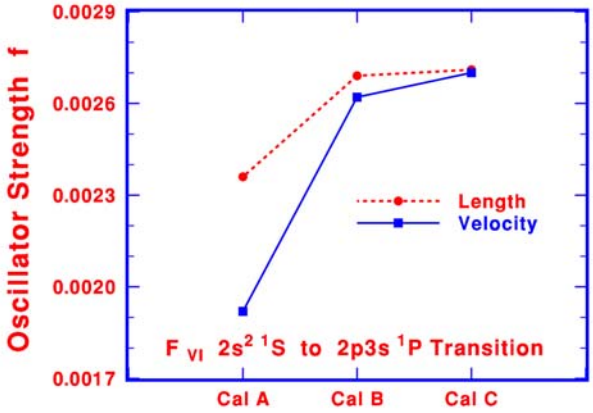

Figure 7. The changes in oscillator strengths for the $2s^2\ ^1S$ to $2p3s\ ^1P$ transitions for F_{VI} from calculations A to C.

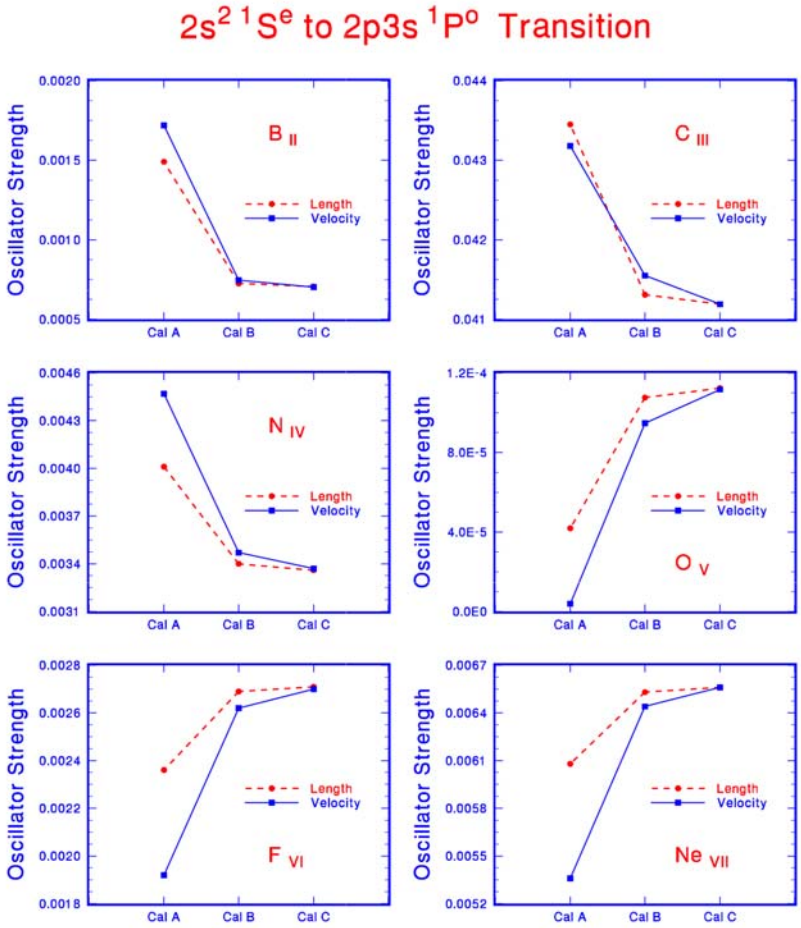

Figure 8. The convergence of the length and velocity results in oscillator strength for the $2s^2\ ^1S$ to $2p3s\ ^1P$ transitions along the Be isoelectronic sequence from calculations A to C.

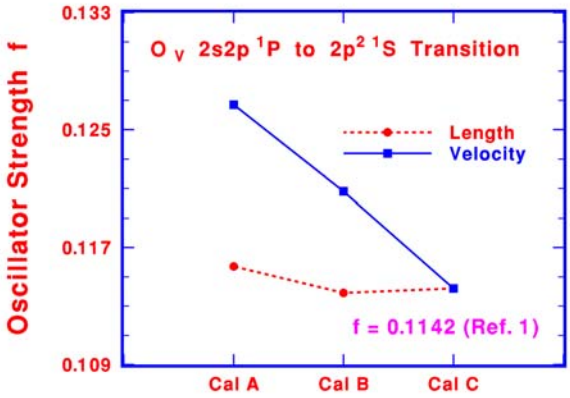

Figure 9. The changes in oscillator strengths for the $2s2p\ ^1P$ to $2p^2\ ^1S$ transitions for O_V from calculations A to C.

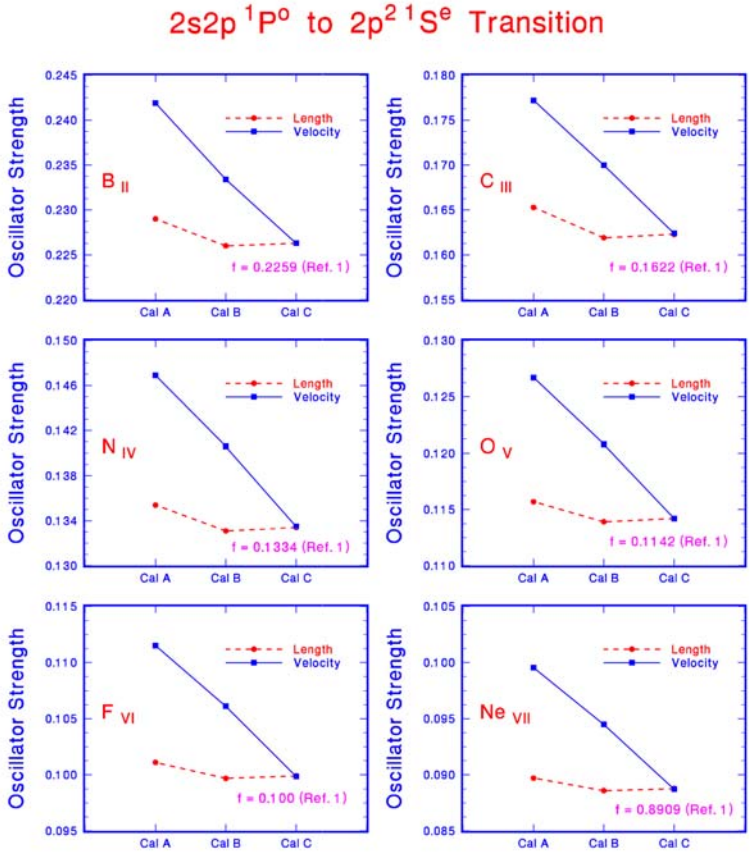

Figure 10. The convergence of the length and velocity results in oscillator strength for the $2s2p\ ^1P$ to $2p^2\ ^1S$ transitions along the Be isoelectronic sequence from calculations A to C. The converged BSCI results are in excellent agreement with the MCHF result [1].

Our third example deals with the transition from a singly excited bound state, $2s2p\ ^1P$, to a doubly excited bound state $2p^2\ ^1S$. Similar to the two transitions we

discussed earlier, this transition is affected by the core-excitation as shown in Fig. 9 by an improvement over the length-velocity agreement in oscillator strength from slightly over 10% to around 6%. The agreement between length and velocity results is further improved to less than 1% when the p^3 effect is taking into account explicitly in our calculation. It is interesting to note that the convergence patterns shown in Fig. 10 for the length and velocity agreement stay the same for all members of the isoelectronic sequence starting from B_{II} where the doubly excited $2p^2\ ^1S$ state first becomes a bound excited state situated between the $2s^2\ ^1S$ ground state and the first singly excited $2s3s\ ^1S$ state shown in Fig. 11. The lack of variation of the convergence patterns shown in Fig. 10 is consistent with the fact that no cross over of the doubly and singly excited states occurs along the isoelectronic sequence, since the $2s2p\ ^1P$ is the lowest bound excited ^1P state (see, e.g., Fig. 5). Again, our calculation has shown that the correction to the velocity results is consistently greater than that of the length results.

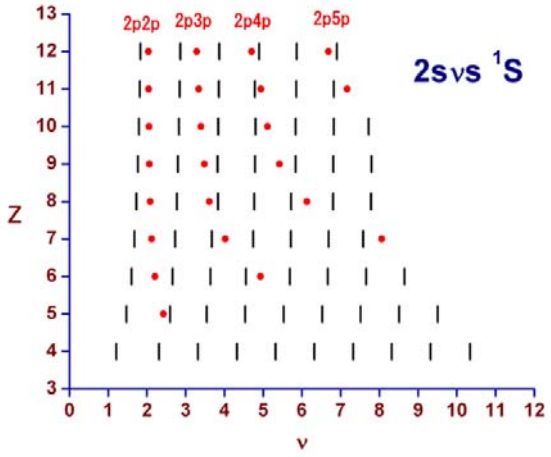

Figure 11. The calculated energy levels in terms of the principal quantum number ν for the singly excited $2sns\ ^1S$ states (vertical bar) and the doubly excited $2pnp\ ^1S$ (solid circle) states for the Be isoelectronic sequence.

Next, we turn our attention to another transition involving the simultaneous change of electronic orbits of the two outer electrons, i.e., the $2p^2\ ^1S \rightarrow 2s3p\ ^1P$ transition. Figure 12 shows that the oscillator strengths are significantly affected by the core-excitation as the difference between the length and velocity results is reduced from around 7% to less than half. This transition is also affected by the p^3 term and it accounts for the further improvement to better than 1% in the length-velocity agreement. Since the relative energy separations between the doubly excited perturbers (i.e., $2p3s\ ^1P$ *vs* $2s3p\ ^1P$ for B_{II}, C_{III} and N_{IV} shown in Fig. 5 and $2s3s\ ^1S$ *vs* $2p^2\ ^1S$ for B_{II} and C_{III} shown in Fig. 11) vary noticeably, the convergence pattern of the length and velocity results for the lower Z members of the isoelectronic sequence are slightly different from that of the high Z members as shown in Fig. 13. The interac-

tions due to the presence of the perturbers both for the initial and the final states of the transition also enhance the oscillator strengths for the few low Z members, which are significantly greater than the oscillator strengths for the higher Z members for this particular transition involving the change of the electronic orbits of two outer electrons. It is interesting to note that, in contrast to the three earlier examples, the core-excitation effects lead to a larger correction to the length result than that for the velocity result for this particular transition. Nevertheless, as expected, the correction due to the p^3 term is essentially limited to the velocity result.

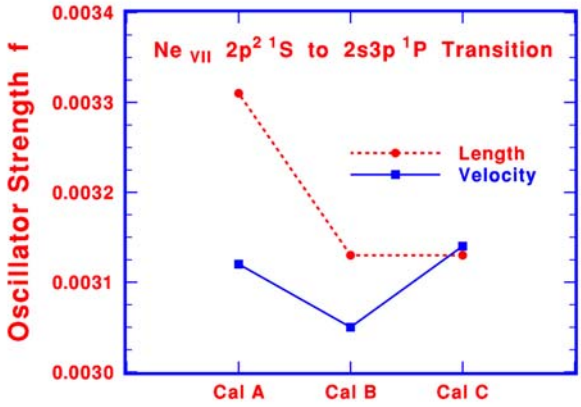

Figure 12. The changes in oscillator strengths for the $2p^2\ ^1S$ to $2s3p\ ^1P$ transitions for Ne_{VII} from calculations A to C.

We will now examine the transitions involving the triplet states. Our first example is the one from the first singly excited triplet state, i.e., the $2s3s\ ^3S$ state to the doubly excited bound $2p3s\ ^3P$ state. Again, we observe the strong core-excitation effect, which leads to a large reduction of the difference between the length and velocity results in oscillator strengths (i.e., from a difference of about 15% to less than 1%) shown in Fig. 14. Our calculation shows little correction due to the p^3 term. This transition involves essentially a single inner $2s$ electron, i.e., the $2s \rightarrow 2p$ transition. The plunges of the doubly excited $2p3s\ ^3P$ state across the singly excited $2snp\ ^3P$ states and also the doubly excited $2p3p\ ^3S$ state across the singly excited $2sns\ ^3S$ states along the isoelectronic sequences of the low Z members (shown in Figs. 15 and 16) do not affect the transition of the inner electron as strong as those involving the outer electrons. As a result, the correction to the oscillator strengths is primarily due to the core-excitation and the convergence patterns of the length and velocity results remain essentially the same along the isoelectronic sequence as shown in Fig. 17. Similar to the singlet transitions discussed earlier, the correction to the velocity results are greater than that for the length results.

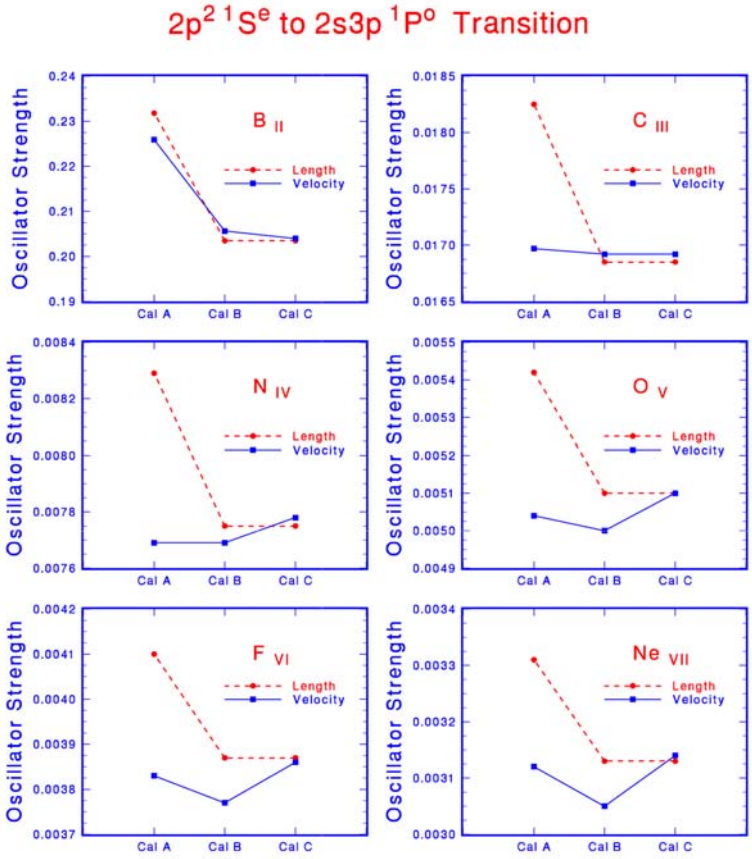

Figure 13. The convergence of the length and velocity results in oscillator strength for the $2p^2\ ^1S$ to $2s3p\ ^1P$ transitions along the Be isoelectronic sequence from calculations A to C.

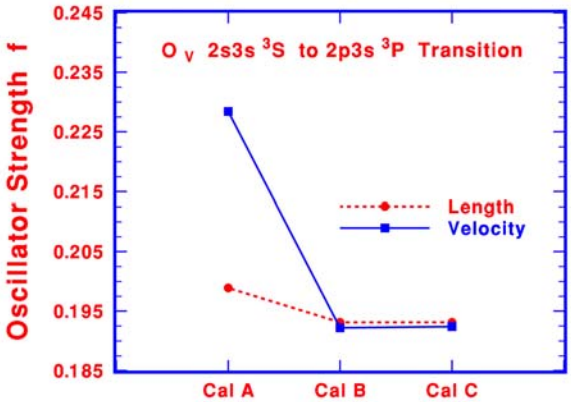

Figure 14. The changes in oscillator strengths for the $2s3s\ ^3S$ to $2p3s\ ^3P$ transitions for O_V from calculations A to C.

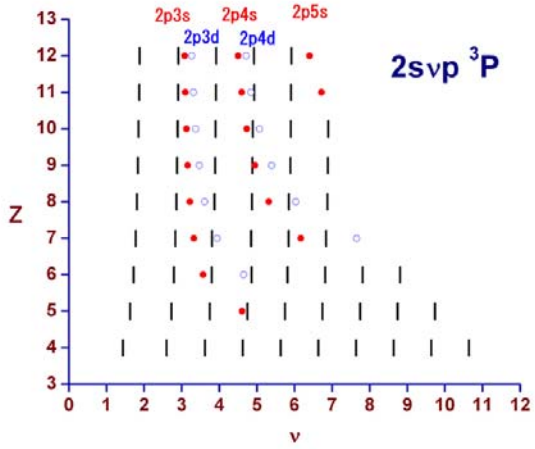

Figure 15. The calculated energy levels in terms of the principal quantum number ν for the singly excited $2snp\ ^3P$ states (vertical bar) and the doubly excited $2pns\ ^3P$ (solid circle) and $2pnd\ ^3P$ (open circle) states for the Be isoelectronic sequence.

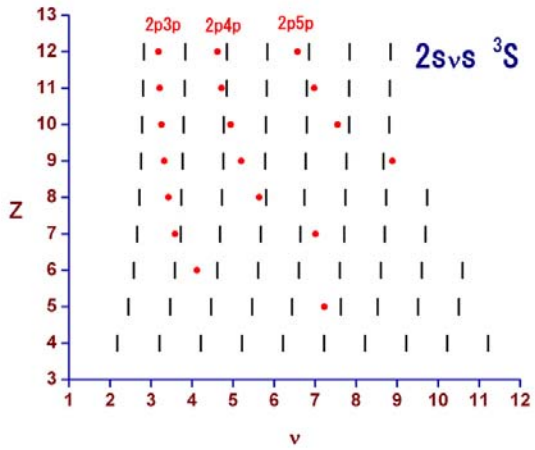

Figure 16. The calculated energy levels in terms of the principal quantum number ν for the singly excited $2sns\ ^3S$ states (vertical bar) and the doubly excited $2pnp\ ^3S$ (solid circle) states for the Be isoelectronic sequence.

Our last example leads us to another transition involving the change of electronic orbits of two outer electrons, i.e., $2s3s\ ^3S \rightarrow 2p3d\ ^3P$ transition. The expected small oscillator strengths for this transition offer another critical test for the precision of the extended BSCI calculation presented in this paper. Similar to other earlier examples, the core-excitation again leads to large corrections (as much as 20% in the velocity calculation) to the oscillator strengths as shown in Fig. 18. The correction due to the p^3 term is again small. The doubly excited $2p3d\ ^3P$ state first become bound in C_{III} as shown in Fig. 15. It is expected that this state is strongly mixed with the singly excited $2s4p\ ^3P$ state of N_{IV} (more than that for the other members of this

isoelectronic sequence) due to their close proximity in energy. As a result, we were not surprised at all when our calculation led to a different length-velocity convergence pattern for N_{IV} as shown in Fig. 19.

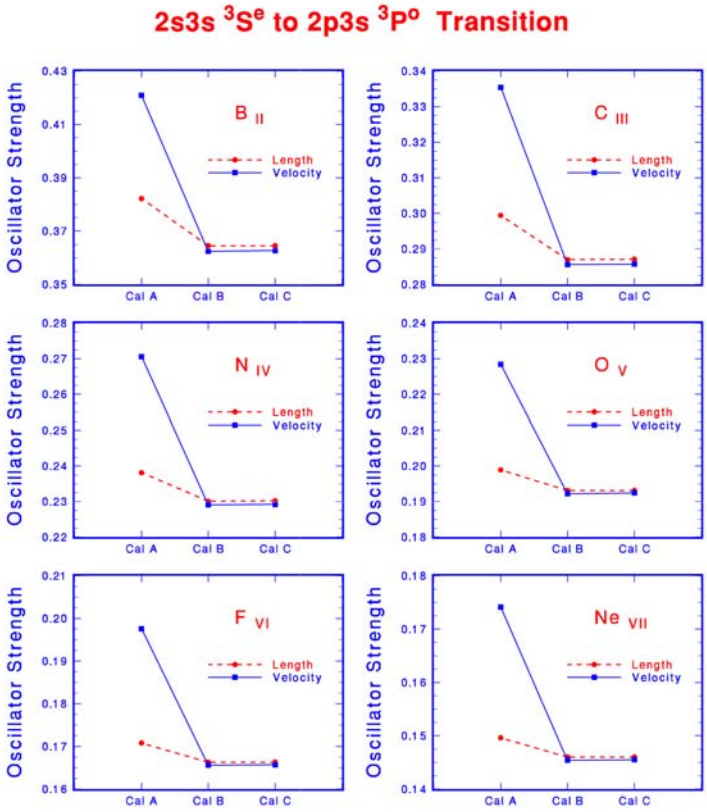

Figure 17. The convergence of the length and velocity results in oscillator strength for the $2s3s\ ^3S$ to $2p3s\ ^3P$ transitions along the Be isoelectronic sequence from calculations A to C.

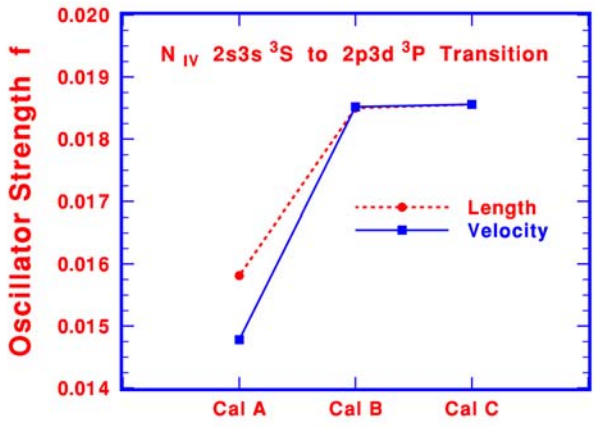

Figure 18. The changes in oscillator strengths for the $2s3s\ ^3S$ to $2p3d\ ^3P$ transitions for N_{IV} from calculations A to C.

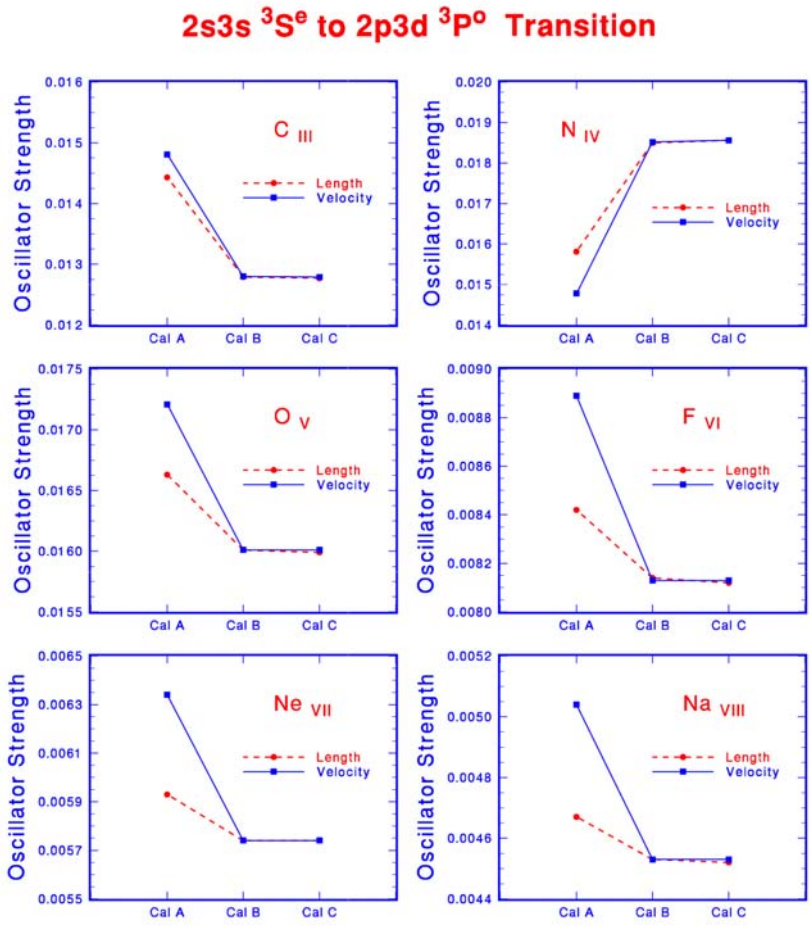

Figure 19. The convergence of the length and velocity results in oscillator strength for the $2s3s\ ^3S$ to $2p3d\ ^3P$ transitions along the Be isoelectronic sequence from calculations A to C.

4. Conclusions

The results reported in this paper have successfully led to definitive answers to the few key questions we asked at the outset. First, the extended BSCI calculation can in fact include the core-excitation effects explicitly in an *ab initio* quantitative estimation of atomic transition data with no need to employ the model potentials. By including in the basis functions configurations corresponding to one of the $1s$ core electrons in an excited electron orbits, i.e., configurations of the type of $([(1snl)^{S_{12}L_{12}}][(n_1l_1n_2l_2)^{S_{34}L_{34}}])^{SL}$, the core-excitation effects are adequately accounted for. Second, the extended BSCI calculation is able to achieve an agreement between the length and velocity results to better than 1% for a large number of transitions involving both singly and doubly excited bound states including states of higher

principal quantum number in a single calculation. Third, with the exception of a few transitions with relatively small oscillator strengths, the correction due to the p^3 term is small in general. The length-velocity agreement is already at the level of 1% or better when the core-excitation interactions are included. Fourth, we have shown quantitatively that the correction to the oscillator strength due to the core-excitation is generally smaller for the length results for most of the transitions discussed in this paper, The correction itself, however, could still be as large as 15-20%, especially for transitions with small oscillator strength. Caution should be exercised when a model potential and the length calculation are employed to estimate the oscillator strength of any atomic transition.

The high performance parallel computing environment has indeed made it possible for the large scale computations required in high precision quantitative studies such as the extended BSCI calculation reported in this paper. Extension of this works in under way for atomic systems such as C_I, where the effect of the p^3 term is expected to be significantly stronger than the one for the 4 electron systems reported in this paper.

Acknowledgments. This work was supported in part by the National Science Council in Taiwan under the grant no. NSC 95-2119-M-007-001 and the HPCC at USC.

References

[1] Tachiev G and Froese Fischer C 1999 *J. Phys. B: At. Mol. Opt. Phys.* **32** 5805

[2] Froese Fischer C, Brage T and Jönsson P 1997 *Computational Atomic Structure - An MCHF Approach* (Bristol: Institute of Physics Publishing)

[3] Chang T N 1993 *Many-body Theory of Atomic Structure and Photoionization* ed Chang T N (Singapore: World Scientific) 213.

[4] Chang T N and Tang X 1991 *Phys. Rev.* A**44** 232

[5] Chang T N and Fang T K 1995 *Phys. Rev.* A**52** 2638

[6] Luo Y 2007 PhD thesis (Los Angeles: Univ So Calif)

[7] Weiss A W 1974 *Phys. Rev.* A**9** 1524; Froese Fischer C and Godefroid M 1982 *Phys. Scr.* **25** 294; Chang T N and Wang R Q 1987 *Phys. Rev.* A**36** 3535